ACS SENSORS

Article

Cite This: ACS Sens. 2019, 4, 1270−1278

pubs.acs.org/acssensors

Amperometric Detection of the Urinary Disease Biomarker *p*-HPA by Allosteric Modulation of a Redox Polymer-Embedded Bacterial Reductase

Somjai Teanphonkrang,[†] Andrzej Ernst,[‡] Salome Janke,[‡] Pimchai Chaiyen,[§] Jeerus Sucharitakul,[∥] Wipa Suginta,[†,§] Panida Khunkaewla,[†] Wolfgang Schuhmann,[‡] Albert Schulte,*[,§] and Adrian Ruff*[,‡]

[†]School of Chemistry, Institute of Science, Biochemistry - Electrochemistry Research Unit (BECRU), Suranaree University of Technology, 30000 Nakhon Ratchasima, Thailand

[‡]Analytical Chemistry - Center for Electrochemical Sciences (CES), Faculty of Chemistry and Biochemistry, Ruhr University Bochum, Universitätsstrasse 150, 44780 Bochum, Germany

[§]School of Biomolecular Science and Engineering (BSE), Vidyasirimedhi Institute of Science and Technology (VISTEC), 21210 Rayong, Thailand

[∥]Department of Biochemistry, Faculty of Dentistry, Chulalongkorn University, 10330 Bangkok, Thailand

Supporting Information

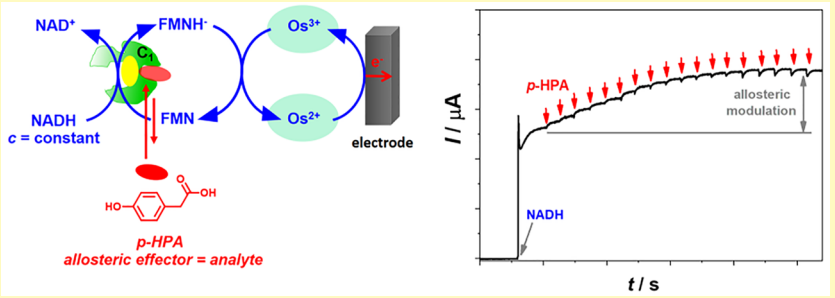

ABSTRACT: We report an amperometric biosensor for the urinary disease biomarker *para*-hydroxyphenylacetate (*p*-HPA) in which the allosteric reductase component of a bacterial hydroxylase, C1-hpah, is electrically wired to glassy carbon electrodes through incorporation into a low-potential Os-complex modified redox polymer. The proposed biosensing strategy depends on allosteric modulation of C1-hpah by the binding of the enzyme activator and analyte *p*-HPA, stimulating oxidation of the cofactor NADH. The pronounced concentration-dependence of allosteric C1-hpah modulation in the presence of a constant concentration of NADH allowed sensitive quantification of the target, *p*-HPA. The specific design of the immobilizing redox polymer with suitably low working potential allowed biosensor operation without the risk of co-oxidation of potentially interfering substances, such as uric acid or ascorbic acid. Optimized sensors were successfully applied for *p*-HPA determination in artificial urine, with good recovery rates and reproducibility and sub-micromolar detection limits. The proposed application of the allosteric enzyme C1-hpah for *p*-HPA trace electroanalysis is the first successful example of simple amperometric redox enzyme/redox polymer biosensing in which the analyte acts as an effector, modulating the activity of an immobilized biocatalyst. A general advantage of the concept of allosterically modulated biosensing is its ability to broaden the range of approachable analytes, through the move from substrate to effector detection.

KEYWORDS: *amperometric biosensing, allosteric modulation, urinary disease biomarker, redox polymers, enzyme electrodes, mediated electron transfer, NADH oxidation, para-hydroxyphenylacetate*

In the human body, *para*-hydroxyphenylacetate (*p*-HPA) is a product of endogenous cellular and opportunistic microbial metabolism of aromatic amino acids. The level of metabolic *p*-HPA formation and the related concentration of this analyte in urine was identified as a reliable indicator for various diseases, ranging from gastrointestinal[1] and toxicological symptoms[2] and intestinal bacterial cell overgrowth (dysbiosis)[3] to neurodegenerative diseases,[4] diabetic nephropathy[5] and gastric cancer.[6] Accordingly, the quantification of this compound and to some extent also its isomers (the *meta*- and *ortho*-compounds) is of particular importance for medical analysis, and straightforward detection schemes for simple on-site monitoring and clinical diagnostics of urinary samples are

Received: January 20, 2019
Accepted: April 10, 2019
Published: April 10, 2019

DOI: 10.1021/acssensors.9b00144
ACS Sens. 2019, 4, 1270−1278

Scheme 1. Schematic of the Proposed Strategy of Allosteric *p*-HPA Biosensing and Molecular Structures of Analyte (*p*-HPA) and the Redox Polymer P(SS-GMA-BA)-Os

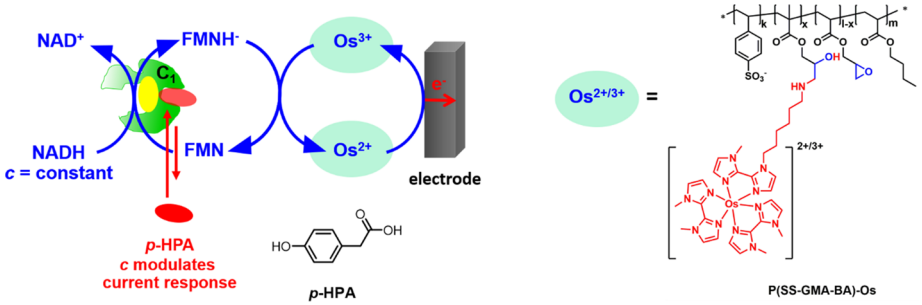

highly desirable. The standard protocols for urinary *p*-HPA identification and quantification include the use of gas chromatography (GC)[7,8] and, more recently, applications of combined techniques such as chromatographic separation (e.g., among others ultrahigh performance liquid chromatography, UHPLC) coupled to mass spectrometry (GC-MS, UHPLC-MS) or electrochemical detection, ^{1}H and ^{13}C nuclear magnetic resonance (NMR) experiments and capillary electrophoresis. In particular, GC-MS was successfully employed as a screening method for varying urinary *p*-HPA in small-bowel disease and bacterial overgrowth syndrome[3,5] and even for the analysis of neonatal urine samples.[9] Complex UHPLC techniques coupled to MS/MS-detection were used to analyze *p*-HPA formation from kaempferol in the investigation of transport mechanisms of metabolites at the intestinal and blood-brain barriers.[10] Furthermore, high resolution ^{1}H NMR analysis was used for quantification of *p*-HPA changes in urinary metabolite profiles[11] and chemical *p*-HPA derivatization allowed the detection of the biomarker by ^{13}C NMR spectroscopy.[12] Finally, high performance liquid chromatography with voltammetric detection in the column eluate was used to assay *p*-HPA in cerebrospinal fluid.[13] All these analytical approaches work well for the quantification of *p*-HPA, but the requirement for time-consuming pretreatment of samples (e.g., derivatization of *p*-HPA[3,14,15]) and the need for rather complex analytical setups are drawbacks to the implementation of easily established and applied (point-of-care) clinical diagnostics.

Purely electrochemical approaches for the detection of *p*-HPA or its derivatives were also considered since these compounds are electroactive and they can be oxidized at suitable anodic potentials. Fast-scan cyclic voltammetry with scan rates of up to 600 V s^{-1} was, for instance, employed to detect *p*-HPA with a carbon fiber microelectrode in tissue samples after stimulation with dopamine.[16] However, the oxidation potential of *p*-HPA is rather high (≈ + 1.0 V vs a pseudoreference Ag/AgCl wire[16]) which might cause interference through electrochemical reactions of other urinary components (e.g., ascorbic acid, paracetamol, or uric acid). Moreover, fast-scan cyclic voltammetry requires special potentiostats, low-noise electrochemical setups and microelectrodes and a high level of operator expertise, rendering such applications unpractical for clinical diagnostics. A recent whole-cell biochemical assay with electrochemical readout involved the voltammetric detection of redox-active pyocyanine, the cellular production rate of which is controlled by *p*-HPA, enabling indirect determination of the target biomarker but with rather low sensitivity and selectivity.[17]

Existing literature examples and successful commercial applications are good evidence that amperometric biosensors with enzymes embedded in polymer layers offer promising selectivity and sensitivity.[18] In the case of biocompatible protein immobilization in adapted hydrophilic redox polymers, biosensors are known to be stable during storage and they can be operated entirely without reagents, which are important characteristics for the construction of a miniaturized device for easy point-of-care biosensing. Recently, we showed that the immobilization of the C1 reductase unit (C1-hpah) of the two-component bacterial *p*-hydroxyphenylacetate 3-hydroxylase (hpah) from *Acetobacter baumannii*[19,20] into an Os-complex-modified polymer was the basis of a NADH biosensor with a sensitivity that could be 1.5-fold enhanced by *p*-HPA, which acts as a molecular effector of C1-hpah that allosterically stimulates the enzymic rate of oxidation of NADH to NAD^{+}.[21] Moreover, preincubation of the polymer/enzyme-modified electrodes in *p*-HPA solution allowed the fabrication of a reagentless sensor device with enhanced NADH detection sensitivity. The observation of allosteric enhancement of the responsiveness of C1-hpah/redox polymer biosensors to NADH was useful for NADH analysis, but since the specific C1-hpah effector *p*-HPA is a urinary disease biomarker and its allosteric effect on NADH oxidation by C1-hpah is highly concentration-dependent, the utilization of C1-hpah/redox polymer biosensors for *p*-HPA analysis is a more important issue from the health care point of view. Thus, proceeding from our previous findings, we adapted here the C1-hpah biosensing scheme for sensitive *p*-HPA determination. In the developed configuration, the current measured with the C1-hpah/redox polymer biosensor reflects the solution concentration of *p*-HPA in the presence of a constant supply of the C1-hpah substrate NADH and is hence suitable for *p*-HPA quantification.

C1-hpah/redox polymer biosensor calibrations and performance tests confirmed that the proposed amperometric biosensor is suitable for the determination of *p*-HPA in samples of known concentration as well as in spiked artificial urine with good recovery rates.

RESULTS AND DISCUSSION

Sensor Concept and Amperometric *p*-HPA Detection.

In our initial work, the optimal current response for NADH detection was achieved with enzyme electrodes that made use of the positively charged polymerPVP-Os (= poly-(vinylpyridine)-$[Os(BiImMe_2)_2(BiImNH_2)]^{3+}$ where $BiImMe_2$ is *N*,*N*′-dimethyl-2,2′-bi-imidazole and $BiImNH_2$ is *N*-(6-aminohexyl)-*N*′-methyl-2,2′-biimidazole), as a low-potential redox polymer matrix for C1-hpah immobilization (redox

DOI: 10.1021/acssensors.9b00144
ACS Sens. 2019, 4, 1270−1278

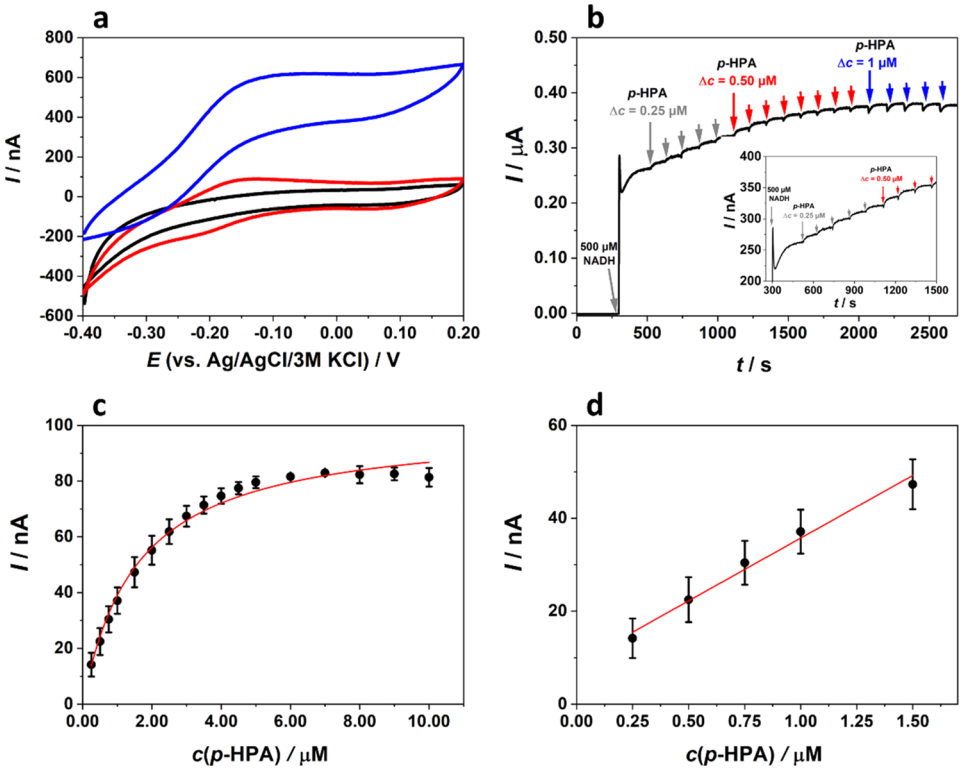

Figure 1. (a) Cyclic voltammetric characterization of a P(SS-GMA-BA)-Os/EDEA/C1-hpah modified glassy carbon electrode (GCE) in 50 mM phosphate buffer, pH 7 with a scan rate of 2 mV s^{-1}. Red trace, c(NADH) = 0; blue trace, c(NADH) = 500 μM; and black trace, background current of an unmodified GCE, measured under identical conditions. (b) Representative chronoamperometric data for a P(SS-GMA-BA)-Os/EDEA/C1-hpah modified GCE, polarized at −100 mV vs Ag/AgCl/3 M KCl; the concentration of *p*-HPA was increased in the presence of 500 μM NADH in incremental steps of 0.25 μM (gray arrows), 0.5 μM (red arrows), and 1 μM (blue arrows) to reach a final value of 10 μM; inset shows a magnification of the first nine additions. (c, d) I−c curves for averaged data from triplicate independent repetitions of chronoamperometric trials as in (b) over the c(*p*-HPA) concentration ranges 0.25−10 μM (c) and 0.25−1.5 μM (d). The red line in (c) corresponds to a curve fit (R^2 = 0.98921) using a Michaels−Menten model for effector binding to the enzyme. The red line in (d) shows the linear fit through the data points in the initial part of the binding curve, where the biosensor response is linear.

potential E of the polymer: E(PVP-Os) = −0.19 V vs Ag/AgCl/3 M KCl).[21]

Although the allosteric effect was less pronounced (1.5-fold increase) compared to solution experiments (20-fold increase[22]), most likely due to steric constraints within the polymer matrix, stable (within the time scale of the experiment) and allosterically responsive polymer/enzyme layers on the surface of graphite electrodes could be formed. For the present application of quantitative *p*-HPA biosensor amperometry, the functional redox polymer was changed to one with an anionic backbone, i.e., P(SS-GMA-BA)-Os (poly(styrenesulfonate-*co*-glycidyl methacrylate-*co*-butyl acrylate)-[$Os(BiImMe_2)_2(BiImNH_2)]^{3+}$, Scheme 1) with E(P(SS-GMA-BA)-Os) = −0.22 V vs Ag/AgCl/3 M KCl. For details of the synthesis and characteristics of the chosen polymer, see ref 21 and the associated Supporting Information. The formal potentials of PVP-Os and P(SS-GMA-BA)-Os are similar (note that the same Os-complex, red part in the molecular structure of the redox polymer shown in Scheme 1, was used for both polymers) and were equally suitable for the required interference-free low potential measurement of enzymic substrate conversion rates.[21] However, compared to previously used PVP-Os, the polymer P(SS-GMA-BA)-Os shows improved stability on glassy carbon electrodes (GCEs) which show low background currents compared to graphite electrodes and were thus employed for all biosensors reported in this contribution.

Moreover, the choice of the P(SS-GMA-BA)-Os matrix that is equipped with an anionic backbone (note that the overall charge of the polymer is positive assuming a triply positively charged Os(III)-complex attached to the GMA monomer, 30 mol %, and single charged sulfonate group in the SS monomer 50 mol %) permitted the use of a high constant NADH concentration at optimal conditions for *p*-HPA detection, resulting in a sustained current and superior sensor stability exhibiting improved allosteric dependence of C1-hpah-driven NADH oxidation on *p*-HPA concentration. We want to emphasize that not only the negative charge at the backbone might influence the film stability in this configuration but also the other comonomers in P(SS-GMA-BA), that is, GMA and BA, which exhibit a rather hydrophobic character that may also contribute to a lower dissolution rate of the polymer/enzyme layers. Moreover, to enhance film stability nucleophilic bifunctional EDEA (= 2,2′-(ethylenedioxy)bis(ethylamine)) was introduced as cross-linker that can react at room temperature with residual electrophilic epoxide groups within the P(SS-GMA-BA) backbone (Scheme 1, blue parts in the molecular structure of the redox polymer; note that this cross-linker was used earlier for the stabilization of polymer/enzyme layers based on the identical polymer backbone[23]).

Figure 1a provides voltammetric proof of P(SS-GMA-BA)-Os/EDEA/C1-hpah redox interaction, while Figure S1a confirms that a significant direct oxidation of NADH did not occur. The contribution of direct electron transfer between the

DOI: 10.1021/acssensors.9b00144
ACS Sens. 2019, 4, 1270−1278

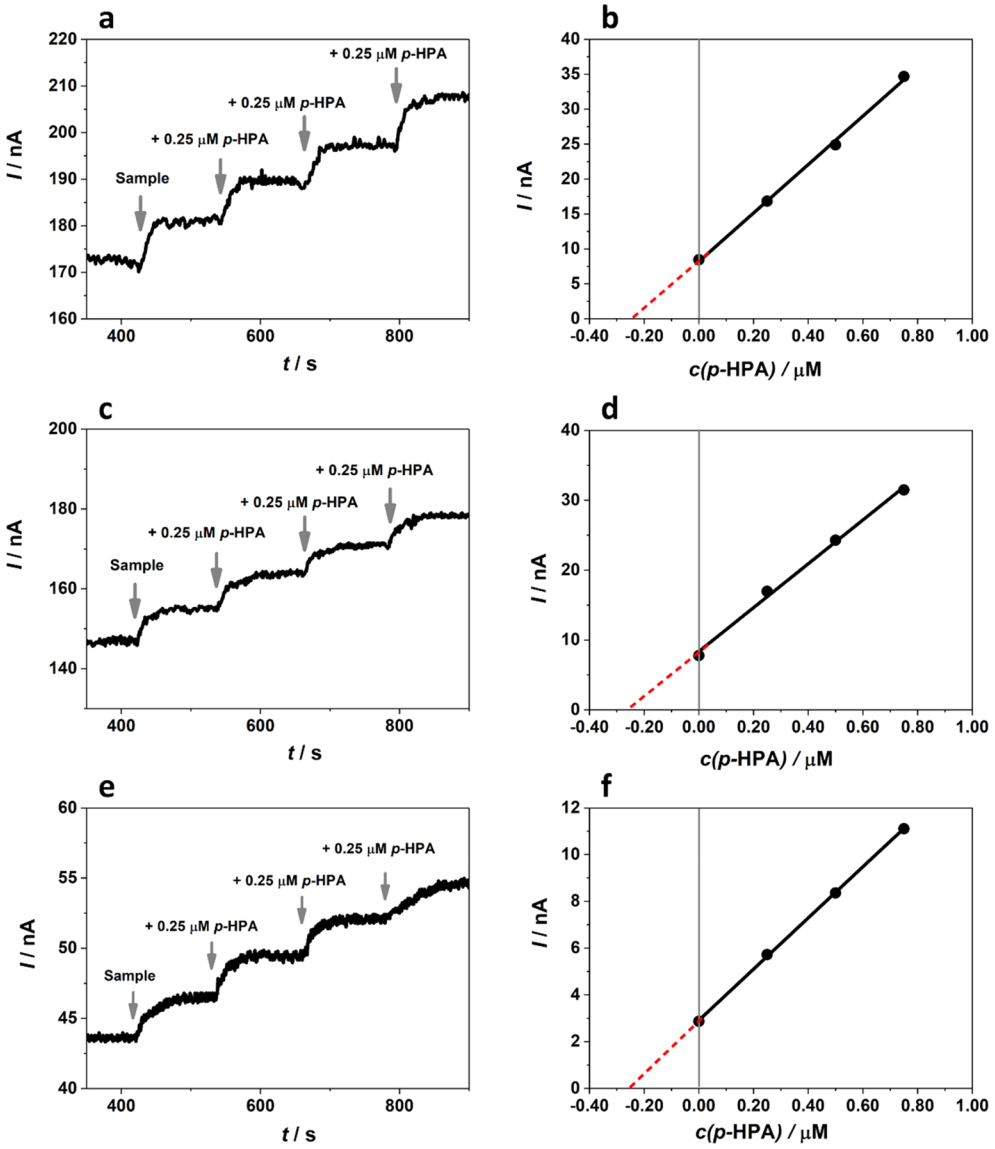

Figure 2. Quantification of *p*-HPA with a P(SS-GMA-BA)-Os/EDEA/C1-hpah modified glassy carbon electrode in 50 mM phosphate, pH 7 (a–d) or artificial urine, pH 7 (e,f) by means of the standard addition method. The NADH concentration was always 500 μM. (a, c, e) Representative chronoamperometric responses of the sensor to addition of the sample and three *p*-HPA standards in incremental steps of 0.25 μM *p*-HPA; (a) sample and *p*-HPA standards are dissolved in phosphate buffer, (c, e) sample and *p*-HPA are dissolved in artificial urine; applied potential −100 mV vs Ag/AgCl/3 M KCl. (b, d, f) Standard addition plots of data extracted from (a, c, e), respectively; the concentrations of the samples were estimated to be 0.236 μM (b), 0.266 μM (d), and 0.266 μM (f), corresponding to recovery rates of 94.4% (b), 106.4% (d), and 106.4% (f). For the linear regressions, R^2 = 0.9981 (b), R^2 = 0.9963 (d), and R^2 = 0.9993 (f).

enzyme and the electrode surface to the oxidative current under NADH turnover conditions was only marginal (Figure S1b).

As shown in Scheme 1, the adaption of the C1-hpah-based NADH biosensor[21] for use in *p*-HPA detection involved quantification of the allosteric modulation of the current induced in a three-electrode biosensor cell with a constant supply of NADH, as a function of analyte (*p*-HPA) concentration. This was achieved by low-noise recording of the amperometric current generated by redox interaction between the NADH-oxidizing enzyme and randomly spread Os-complexes in the polymer network. Accurate *p*-HPA quantification then depends on reliable scaling of the biosensor current with increasing *p*-HPA concentration, either in electrolytes supplemented with known concentrations of the compound or for samples using the standard addition method, with aliquots of sample solution and a series of *p*-HPA standards added.

To test the feasibility of the approach as shown in Scheme 1, chronoamperometric measurements were conducted with triplicates of P(SS-GMA-BA)-Os/EDEA/C1-hpah-modified GCEs at −100 mV vs Ag/AgCl/3 M KCl in phosphate-buffer (50 mM, pH 7) supplemented with 500 μM NADH and with different levels of added *p*-HPA. As shown in the representative current trace (Figure 1b), the NADH oxidation current is enhanced upon addition of *p*-HPA, reflecting allosteric modulation of C1-hpah. Individual current elevations above the nonstimulated baseline level in response to five 0.25 μM (gray arrows), eight 0.50 μM (red arrows), and five 1.00 μM (blue arrows) activator increments were derived from the three identically prepared P(SS-GMA-BA)-Os/EDEA/C1-hpah biosensors from the same batch, averaged and then plotted as a

DOI: 10.1021/acssensors.9b00144
ACS Sens. 2019, 4, 1270–1278

Table 1. Detection of *p*-HPA in 50 mM Phosphate Buffer (PB, pH 7) or Artificial Urine (AU, pH 7 and 8)[a]

			c(*p*-HPA)/μM			
entry	working electrolyte	*p*-HPA in	adjusted	found	recovery rate/%	sensitivity/nA μM^{-1}
1	PB, pH 7	PB, pH 7	0.25	(0.24 ± 0.01)	(95 ± 4)	(26 ± 5)
2	PB, pH 7	AU, pH 7	0.25	(0.25 ± 0.01)	(101 ± 5)	(24 ± 7)
3	AU, pH 7	AU, pH 7	0.25	(0.26 ± 0.02)	(103 ± 7)	(20 ± 5)
4	AU, pH 8	AU, pH 8	0.25	(0.26 ± 0.01)	(106 ± 2)	(20 ± 7)

[a]The solution concentration of *p*-HPA was adjusted to a nominal 0.250 μM, with three subsequent standard additions. The initial adjusted sample concentration was estimated from the $I-c$ plots of measurements with the standard addition method at I = 0 A by linear regression through the individual data points. Sensitivities were derived from the slope of the $I-c$ plots. Note that the concentrations were adjusted to be within the linear detection range of the sensor. Applied potential for all experiments was −100 mV vs Ag/AgCl/3 M KCl.

function of the concentration of the allosteric effector (Figure 1c).

At low *p*-HPA concentrations current values increased rapidly and linearly with the effector concentration but reached a plateau at high effector level. This curve shape was predictable since allosteric C1-hpah modulation occurs by binding of *p*-HPA to a limited number of sites on the enzyme surface, which becomes saturated as the *p*-HPA concentration increases. Fitting the *I-c* data from Figure 1c with the function for Michaels Menten-type binding to a single type of binding-site (red line in Figure 1c) yielded an apparent K_m value of (1.6 ± 0.1) μM. Saturation occurred at *p*-HPA concentrations >5 μM, while the linear range of the current response for *p*-HPA detection extended to about 1.5 μM (Figure 1d) and the average sensitivity of the tested sensor electrodes was (27 ± 2) nA μM^{-1} *p*-HPA. These characteristics were valuable first indications of the suitability of allosteric enzyme/redox polymer biosensor arrangements for the analysis of particular enzyme effector concentrations.

It is worth mentioning here that using NADH concentrations lower than 500 μM produced a current response that declined over time and was therefore unsuitable for proper *p*-HPA quantification (Figure S2). We should also emphasize that, in *p*-HPA detection mode (constant NADH concentration, varying *p*-HPA concentration), C1-hpah immobilization layers prepared with PVP-Os did not show a stable current response over the time scale of the experiment (Figure S3). With low NADH concentrations the sensor current was reasonably stable in the absence of *p*-HPA but decreased upon addition of the allosteric effector (Figure S3a and b). With higher NADH concentrations, the decrease in current was observed even in the absence of *p*-HPA (Figure S3c). Apparently, exposure to high concentrations of NADH destabilizes the polymer/enzyme film and induces desorption during amperometric detection (note that in our previous work only NADH concentrations ≤ 500 μM were employed[21]). For lower NADH concentrations, accumulation of the substrate leading to desorption of the film upon *p*-HPA addition might occur. However, with *p*-HPA present and subsequent addition of NADH to the solution (NADH detection mode), this effect is absent. We conclude that the sequence of reagent addition for operating the sensor either in NADH or *p*-HPA detection mode is of particular importance. Cofactor degradation, which is known to occur in phosphate containing media[24,25] does not seem to be an issue within the time scale of experiments that were performed under optimized conditions. A disturbing current decrease in typical chronoamperometric trials was not observed.

To evaluate their performance in quantitative *p*-HPA analysis, P(SS-GMA-BA)-Os-modified GCEs were used in a series of analytical trials, with the target analyte dissolved either in phosphate buffer or in artificial urine and measurements by the standard addition method in either phosphate buffer or artificial urine of various pH as supporting electrolyte. Figure 2a shows a representative chronoamperometric response for a sample in phosphate buffer measured with the standard addition method with a P(SS-GMA-BA)-Os-modified GCE at a constant NADH concentration of 500 μM. From the corresponding standard addition plot (Figure 2b) the *p*-HPA concentration was determined to be 0.236 μM, which corresponds to a recovery rate of 94.4% for the 0.25 μM sample. The standard addition method was selected for quantitative *p*-HPA analysis since its inherent internal calibration minimizes/fully excludes within individual sample runs the errors that might originate from sample matrix effects and/or slight variations in sensor performance. The mean values for the estimated concentrations and recoveries, calculated for seven independent *p*-HPA quantifications (Table S1), were estimated to be (0.24 ± 0.01) μM and (95 ± 4)% (Table 1, entry 1).

The observed small standard deviations confirmed the satisfactory reproducibility of the electrode construction. Moreover, the results obtained with the standard addition method and the test runs shown in Figure 1 were conducted with sensors containing redox polymers from different batches; however, the average sensitivity determined from the seven independent experiments (note that the standard addition experiments were conducted within the linear response of the sensors) was (26 ± 5) nA μM^{-1} which is statistically indistinguishable from the value measured with the first polymer batch ((27 ± 2) nA μM^{-1}). The limit of detection for samples prepared and measured in phosphate buffer was derived to be 0.038 μM from the standard deviation of the background current response (in the absence of NADH and *p*-HPA) and the average sensitivity. This is in the same range as the value reported for the direct electrochemical detection of *p*-HPA by fast scan cyclic voltammetry (0.1 μM).[16] Amperometric biosensor detection of *p*-HPA with a signal dependent on the allosteric effect of the analyte on redox polymer-embedded C1 reductase is both reproducible and reliable.

Detection of *p*-HPA in Artificial Urine Samples. Since *p*-HPA is an important urinary disease biomarker we evaluated the suitability of the proposed sensor scheme for quantification of the target analyte in artificial urine samples using the standard addition method (for the composition of the artificial urine see Table S2 and/or ref 26). Figure 2c shows the chronoamperometric response with a P(SS-GMA-BA)-Os/EDEA/C1-hpah-modified electrode in deaerated phosphate buffer (50 mM, pH 7) to which first an aliquot of an artificial urine solution (pH 7) containing 0.25 μM *p*-HPA (the

DOI: 10.1021/acssensors.9b00144
ACS Sens. 2019, 4, 1270−1278

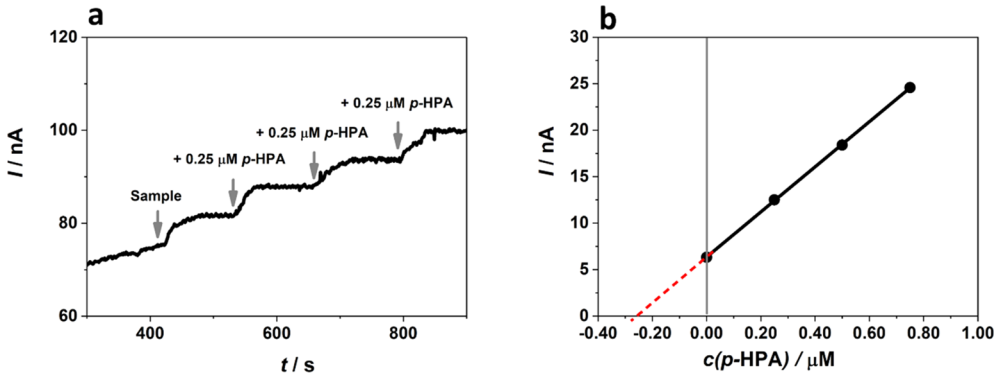

Figure 3. Quantification of *p*-HPA with a P(SS-GMA-BA)-Os/EDEA/C1-hpah-modified glassy carbon electrode in artificial urine with an adjusted pH value of 8 and containing 500 μM NADH by means of the standard addition method. (a) Representative chronoamperometric response of the sensor to addition of the sample (nominal concentration of 0.25 μM) and the three *p*-HPA standards in incremental steps of 0.25 μM *p*-HPA; sample and *p*-HPA standards were dissolved in artificial urine (pH 8); the applied potential was −100 mV vs Ag/AgCl/3 M KCl. (b) Standard addition plot obtained for data extracted from (a); the concentration of the samples was estimated to be 0.262 μM, corresponding to a recovery of 104.8%, from the intercept of the linear regression, R^2 = 0.9999.

sample) and subsequently three aliquots of standard *p*-HPA solution were added. From the linear regression of the *I*−*c* plot (Figure 2d) the concentration of the sample was determined to be 0.266 μM, corresponding to a recovery of 106.4% of the nominal sample concentration, 0.25 μM. The mean value of the determined concentration and the recovery rate over eight independent measurements (Table S3) were calculated to be (0.25 ± 0.01) μM and (101 ± 5)%, respectively (Table 1, entry 2).

The mean sensitivity derived from the three independent experiments was (24 ± 7) nA μM^{-1}, which is in good agreement with that in pure phosphate buffer. We conclude that addition of artificial urine (pH 7) samples has no effects on the performance of the biosensor. This is supported by the fact that addition of artificial urine at the end of a standard addition experiment had no effect on the steady state current (Figure S4).

With this result and aiming for a clinical device that could be used directly for measurements in the sample matrix, i.e., in urine, we examined the applicability of the developed sensor to direct quantification of *p*-HPA in artificial urine, without using any background electrolyte or buffer system for dilution. Artificial urine contains salts such as NaCl (90 mM) and NH_4Cl (25 mM) in rather high concentrations (Table S2), and consequently the addition of an external supporting electrolyte is unnecessary. Moreover, the low-potential polymer-bound Os-complex that ensures an operational potential of −100 mV vs Ag/AgCl/3 M KCl should exclude unwanted side-reactions such as the co-oxidation of uric acid (0.4 mM) or other redox-active components of the sample solution.

Figure 2e depicts the chronoamperometric response during a standard addition measurement conducted in artificial urine (pH 7) as supporting electrolyte. The analyte sample (nominal concentration = 0.25 μM) was first added to the solution, followed by three standard additions that increased the *p*-HPA concentration in steps of 0.25 μM. Quantitative analysis (Figure 2f) yielded a sample concentration of 0.266 μM, corresponding to a recovery rate of 106.40%. Mean values for the concentration, recovery and sensitivity over four independent standard additions (Table S4) were (0.26 ± 0.02) μM, (103 ± 7)%, and (20 ± 5) nA μM^{-1}, respectively (Table 1, entry 3). The slightly lower sensitivity might be due to the impact of the artificial urine on the polymer matrix. The limit of detection in artificial urine was calculated to be 0.164 μM, which is slightly higher than in pure phosphate buffer, indicating the matrix effect. However, our results unambiguously demonstrate that quantification of *p*-HPA in artificial urine with the proposed sensor scheme is possible in a reproducible and reliable manner.

Evidently, the high selectivity of the C1-hpah reductase component of *p*-HPA hydroxylase ensures a straightforward measurement protocol for the quantification of the urinary disease biomarker *p*-HPA that circumvents complex sample pretreatments such as derivatization (NMR) or separation (HPLC).

In the medical diagnostic literature the *p*-HPA content of urine is generally reported relative to the creatinine content, as micrograms of *p*-HPA per gram of creatinine, since creatinine excretion is relatively constant and unaffected by changes in metabolism.[11,27] The detection limit in artificial urine (0.164 μM or 25 $\mu g\ L^{-1}$ with a molecular weight of *p*-HPA of 152.15 g mol^{-1}), referenced to the adjusted model creatinine level (7 mM or 0.8 g L^{-1}, Table S2), was estimated to be 31 μg (g creatinine)$^{-1}$, which is within the reported range of the *p*-HPA content of normal urine (21−52 μg (g creatinine)$^{-1}$, as measured by GC-MS[8]) and comparable to detection ranges with other more complex techniques such as NMR.[11]

Effect of the pH Value on Biosensor Performance. Since the pH value of urine may vary, depending on the human subject's state of health, nutrition, fluid uptake, or ingestion of drugs,[26] and the C1-component shows a rather constant activity within a pH range of 6.0−8.0 (see Experimental Section), we further evaluated the operational pH-window of the proposed sensor by carrying out *p*-HPA quantification at various pH values, i.e., under slightly basic (pH 8) and acidic conditions (pH 6.6). As can be seen in Figure 3a, chronoamperometric *p*-HPA measurements in artificial urine at pH 8 (adjusted by adding appropriate amounts of 6 M NaOH) show a reasonably stable current output in the absence and presence of the analyte *p*-HPA (note that measurements at pH 8 in 50 mM phosphate buffer show the same trend, Figure S5a).

Mean values from four independent standard addition experiments (Table S5) determined from the corresponding *I*−*c* plots (Figure 3b) were (0.26 ± 0.01) μM and (106 ± 2)%,

DOI: 10.1021/acssensors.9b00144
ACS Sens. 2019, 4, 1270−1278

for the concentration and the corresponding recovery, respectively. The sensitivity for the biosensor operation at pH 8 was estimated to be (20 ± 7) nA μM^{-1}. Apparently, both values are slightly smaller than the values obtained in phosphate buffer of the same pH, indicating a small influence of the measuring environment on sensor performance. However, since the standard deviations for the different conditions are overlapping, the effect is insignificant.

In contrast, standard addition measurements in artificial urine at pH 6.6 (adjusted by adding appropriate aliquots of 6 M aqueous HCl) were unsuccessful, as a continuous decrease of the current response was observed even before electrolyte supplementation with the analyte (Figure S5b). Thus, quantification in urine of this acidity was not possible with the proposed detection scheme. Moreover, biosensor operation in 50 mM phosphate buffer of pH 6.6 did not show any significant current response. Loss of function at the lower pH value is likely to be due to a decrease of C1-hpah activity in the immobilized/polymer-embedded state (note that the decrease in solution is only little, see Experimental Section) and, though to lesser extent, to a reduced hydrophilicity of the polymer film due to partial protonation of the sulfonate groups. However, in this electrolyte the initial current is significantly lower than that obtained in artificial urine. We therefore conclude that not only effects on the polymer matrix are responsible for the poor current response at this pH value, but that the low pH value itself causes this effect.

CONCLUSION

We present, for the first time, an amperometric biosensor for the urinary disease biomarker *p*-HPA based on allosteric modulation of the bacterial reductase C1 embedded and electrically wired to the electrode surface in a redox hydrogel. Modulation by the analyte *p*-HPA of the sensor current observed at a constant NADH supply allowed quantification of the biomarker. C1-hpah/redox polymer biosensors showed reproducible analytical performance and offered a linear detection range of 0.25−1.5 μM.

Moreover, the benefits that were gained from combining the selective allosteric biorecognition element with a low potential redox polymer enabled reliable detection of *p*-HPA in artificial urine and was not hampered by effects on the polymer matrix or adverse signal disturbance due to the electrochemical co-oxidation of potentially interfering substances such as uric acid, under neutral and slightly basic conditions. However, at weakly acidic conditions commonly found in the urine of a healthy humans (≈6), the detection of *p*-HPA was hindered due to instability of the biosensor current, even in the absence of the analyte.

Our results clearly demonstrate that the detection of the urinary disease biomarker *p*-HPA directly in urine is possible under appropriate conditions of pH, which can easily be arranged by pH-adjustment before analysis. Thus, our proposed sensor concept is promising for the fabrication of straightforward diagnostics devices for the detection of the urinary disease biomarker *p*-HPA, and, with a change in the entrapped allosteric enzyme, for other relevant biomarkers, too.

Operation of the methodology on mass-fabricated screen printed electrode platforms together with the establishment of a glucose meter-like signal readout via hand-held electronic devices and the realization of success with use of the precalibration instead of standard addition method may ultimately allow even the accomplishment of tools for point-of-care *p*-HPA testing in hospitals and rapid *p*-HPA screens at the doctor's office or at home.

EXPERIMENTAL SECTION

Materials and Methods. All chemicals and materials were purchased from Sigma-Aldrich, VWR, Alfa-Aesar or Acros Organics and were of reagent or higher grade. All aqueous buffer and stock solutions were prepared with ultrapure deionized water from a Milli-Q water purification system. Synthesis of the redox polymer poly(4-styrenesulfonate-*co*-glycidyl methacrylate-cobutyl acrylate)-[Os-$(BiImMe_2)_2(BiImNH_2)]^{3+}$ (P(SS-GMA-BA)-Os, with $BiImMe_2$ = *N*,*N*′-dimethyl-2,2′-biimidazole and $BiImNH_2$ = *N*-(6-aminohexyl)-*N*′-methyl-2,2′-biimidazole) was described previously.[21] However, for $BiImMe_2$ and $[Os(BiImMe_2)Cl_2]PF_6$ involved in the preparation of the Os-complex $[Os(BiImMe_2)_2(BiImNH_2)](PF_6)_3$, optimized synthesis procedures were used, which shortened the reaction time significantly (see Supporting Information for details). The optimized preparation protocol of the bidentate ligand $BiImMe_2$ was adapted from a reported procedure for the alkylation of imidazole derivatives.[28] The Os-complex precursor $[Os(BiImMe_2)Cl_2]PF_6$ was prepared following procedures reported in ref 29, All other reactions were conducted as described previously.[21] The polymer has a redox potential of −220 mV and a nominal composition of SS = 50 mol %, GMA = 30 mol % and BA = 20 mol %. P(SS-GMA-BA)-Os was used as an aqueous solution with a concentration of 9.75 mg mL^{-1}. The bifunctional diamine 2,2′-(ethylenedioxy)bis(ethylamine) (EDEA) was used as a cross-linker for polymer film formation, as an aqueous solution of concentration 40.8 mg mL^{-1}. The coenzyme β-nicotinamide adenine dinucleotide (NADH, reduced form, disodium salt hydrate) and the allosteric effector *para*-hydroxyphenylacetate (*p*-HPA) were purchased from Acros Organics. Stock solutions of NADH (50 mM) were made in Tris-Cl buffer (10 mM, pH 10) and stored at 4 °C. Stock solutions of *p*-HPA (50 μM) were made in sodium phosphate buffer (50 mM, pH 7) or artificial urine (pH 6.6, 7 or 8). Artificial urine was prepared following the formulation of Brooks et al.;[26] for the exact composition, refer to Table S2.

Enzyme. The C1 reductase (C1-hpah) component of *p*-hydroxyphenylacetate hydroxylase from *A. baumannii* was expressed and purified according to protocols described earlier in refs 19 and 20. Stock solutions of C1-hpah were prepared in 50 mM phosphate buffer (pH 7) at a concentration of 36.4 mg mL^{-1} and stored at −20 °C. The activity of C1-hpah in solution at various pH values was estimated in 50 mM sodium phosphate pH 6.0, 6.6, 7.0, and 8.0 at 25 °C and in the presence of 200 μM NADH, 1 mM HPA and 0.1 μM of the C1 reductase component to be 0.077 $\mu M\ s^{-1}$(pH 6.0), 0.084 $\mu M\ s^{-1}$ (pH 6.6), 0.110 $\mu M\ s^{-1}$ (pH 7.0) and 0.082 $\mu M\ s^{-1}$ (pH 8.0).

Electrochemical Experiments. All electrochemical experiments were conducted in a standard three-electrode electrochemical cell (working volume, approximately 4 mL) with a Pt wire acting as counter-electrode and a Ag/AgCl/3 M KCl reference electrode. Polymer/enzyme modified glassy carbon electrodes (3 mm diameter, sealed in PEEK or Teflon, BAS Instruments) were employed as working electrodes. Before chemical modification, the glassy carbon electrodes were polished with alumina of grain size 0.5 μm. All experiments were conducted in 50 mM phosphate buffer solution or artificial urine[26] (for pH, see text), deaerated by Ar or N_2 bubbling for 30 min, under an argon or nitrogen atmosphere using a CHI 1030 multichannel potentiostat, a PalmSens3 potentiostat or a Gamry Ref600 potentiostat. All chronoamperometric experiments were performed with an applied potential of −100 mV vs Ag/AgCl/3 M KCl. All data points in calibration graphs correspond to averaged background-corrected currents measured in multiplicate trials with the corresponding type of polymer/enzyme electrode. Limit of detection (LOD) was calculated as LOD = (3 × standard deviation of the background)/sensitivity. Analyte concentrations in artificial urine were calculated with respect to the adjusted creatinine concentration in this electrolyte, which was 7 mM, or expressed as mass concentration, 0.8 g L^{-1}(see Table S2).

DOI: 10.1021/acssensors.9b00144
ACS Sens. 2019, 4, 1270−1278

Electrode Modification. All polymer/enzyme electrodes were prepared by drop-casting using stock solutions of P(SS-GMA-BA)-Os (9.75 mg mL^{-1} in water), C1-hpah (36.4 mg mL^{-1} in 50 mM phosphate, pH 7), and EDEA (40.8 mg mL^{-1} in water). For electrode surface modification, the enzyme, polymer, and cross-linker solution were mixed in a mass ratio of 4.38:2.88:1 (the optimal condition, obtained by testing several ratios, corresponds to the following concentrations: P(SS-GMA-BA)-Os = 7.20 mg mL^{-1}; C1-hpah = 10.95 mg mL^{-1}; EDEA = 2.5 mg mL^{-1} in the final solution) and 5 μL of this mixture was used for the modification of a single glassy carbon electrode. The film was dried for 2 h at room temperature and then stored at 4 °C until use.

■ ASSOCIATED CONTENT

Supporting Information

The Supporting Information is available free of charge on the ACS Publications website at DOI: 10.1021/acssensors.9b00144.

Additional electrochemical experiments, synthetic protocols, controls, and additional sensor characteristics (PDF)

■ AUTHOR INFORMATION

Corresponding Authors

*(A.S.) Tel.: +66-8737-58518. E-mail: albert.s@vistec.ac.th.
*(A.R.) Tel.: +49-234-3225586. E-mail: adrian.ruff@rub.de.

ORCID

Wipa Suginta: 0000-0001-5927-7192
Wolfgang Schuhmann: 0000-0003-2916-5223
Albert Schulte: 0000-0002-3034-6075
Adrian Ruff: 0000-0001-5659-8556

Notes

The authors declare no competing financial interest.

■ ACKNOWLEDGMENTS

We acknowledge the core financial support of this work by the Thailand Research Fund through a grant from the respected Royal Golden Jubilee Ph.D. Program (Grant No. PHD/0160/2557 to S.T. and Grant No. RTA5980007) and by the Suranaree University of Technology through supportive budget allocations to W.S., A.S. and P.K. and their Biochemistry-Electrochemistry Research Unit. W.S. and A.R. thank the Deutsche Forschungsgemeinschaft (DFG, German Research Foundation) under Germany's Excellence Strategy – EXC-2033–project number 390677874 for a PostDoc fellowship for A.R. Research in the P.C. laboratory was financially supported by a grant from the Thailand Research Fund (RTA5980001) and VISTEC. Thanks also to Dr David Apps, School of Medicine, University of Edinburgh, for comments on the manuscript and for language improvements.

■ REFERENCES

(1) Sarosiek, I.; Schicho, R.; Blandon, P.; Bashashati, M. Urinary metabolites as noninvasive biomarkers of gastrointestinal diseases: A clinical review. *WJGO* **2016**, *8*, 459–465.

(2) Lord, R. S.; Bralley, J. A. Clinical applications of urinary organic acids. Part I: Detoxification markers. *Altern. Med. Rev.* **2008**, *13*, 205–215.

(3) Chalmers, R. A.; Valman, H. B.; Liberman, M. M. Measurement of 4-hydroxyphenylacetic aciduria as a screening test for small-bowel disease. *Clin. Chem.* **1979**, *25*, 1791–1794.

(4) An, M.; Gao, Y. Urinary Biomarkers of Brain Diseases. *Genomics, Proteomics Bioinf.* **2015**, *13*, 345–354.

(5) Stec, D. F.; Wang, S.; Stothers, C.; Avance, J.; Denson, D.; Harris, R.; Voziyan, P. Alterations of urinary metabolite profile in model diabetic nephropathy. *Biochem. Biophys. Res. Commun.* **2015**, *456*, 610–614.

(6) Jung, J.; Jung, Y.; Bang, E. J.; Cho, S.-i.; Jang, Y.-J.; Kwak, J.-M.; Ryu, D. H.; Park, S.; Hwang, G.-S. Noninvasive diagnosis and evaluation of curative surgery for gastric cancer by using NMR-based metabolomic profiling. *Ann. Surg. Oncol.* **2014**, *21* (Suppl4), S736–42.

(7) Chalmers, R. A.; Healy, M. J.; Lawson, A. M.; Hart, J. T.; Watts, R. W. Urinary organic acids in man. III. Quantitative ranges and patterns of excretion in a normal population. *Clin. Chem.* **1976**, *22*, 1292–1298.

(8) Tanaka, K.; West-Dull, A.; Hine, D. G.; Lynn, T. B.; Lowe, T. Gas-chromatographic method of analysis for urinary organic acids. II. Description of the procedure, and its application to diagnosis of patients with organic acidurias. *Clin. Chem.* **1980**, *26*, 1847–1853.

(9) Hoehn, T.; Janssen, S.; Mani, A. R.; Brauers, G.; Moore, K. P.; Schadewaldt, P.; Mayatepek, E. Urinary excretion of the nitrotyrosine metabolite 3-nitro-4-hydroxyphenylacetic acid in preterm and term infants. *Neonatology* **2008**, *93*, 73–76.

(10) Moradi-Afrapoli, F.; Oufir, M.; Walter, F. R.; Deli, M. A.; Smiesko, M.; Zabela, V.; Butterweck, V.; Hamburger, M. Validation of UHPLC-MS/MS methods for the determination of kaempferol and its metabolite 4-hydroxyphenyl acetic acid, and application to in vitro blood-brain barrier and intestinal drug permeability studies. *J. Pharm. Biomed. Anal.* **2016**, *128*, 264–274.

(11) Saude, E. J.; Adamko, D.; Rowe, B. H.; Marrie, T.; Sykes, B. D. Variation of metabolites in normal human urine. *Metabolomics* **2007**, *3*, 439–451.

(12) Shanaiah, N.; Desilva, M. A.; Nagana Gowda, G. A.; Raftery, M. A.; Hainline, B. E.; Raftery, D. Class selection of amino acid metabolites in body fluids using chemical derivatization and their enhanced 13C NMR. *Proc. Natl. Acad. Sci. U. S. A.* **2007**, *104*, 11540–11544.

(13) Kobayashi, K.; Koide, Y.; Shohmori, T. Determination of p-hydroxyphenylacetic acid in cerebrospinal fluid by high-performance liquid chromatography with electrochemical detection. *Clin. Chim. Acta* **1982**, *123*, 161–168.

(14) Hoffmann, G.; Aramaki, S.; Blum-Hoffmann, E.; Nyhan, W. L.; Sweetman, L. Quantitative analysis for organic acids in biological samples: Batch isolation followed by gas chromatographic-mass spectrometric analysis. *Clin. Chem.* **1989**, *35*, 587–595.

(15) Hušek, P.; Švagera, Z.; Hanzlíková, D.; Řimnáčová, L.; Zahradníčková, H.; Opekarová, I.; Šimek, P. Profiling of urinary amino-carboxylic metabolites by in-situ heptafluorobutyl chloroformate mediated sample preparation and gas chromatography-mass spectrometry. *J. Chromatogr. A* **2016**, *1443*, 211–232.

(16) Shin, M.; Kaplan, S. V.; Raider, K. D.; Johnson, M. A. Simultaneous measurement and quantitation of 4-hydroxyphenylacetic acid and dopamine with fast-scan cyclic voltammetry. *Analyst* **2015**, *140*, 3039–3047.

(17) Dierckx, S.; van Puyvelde, S.; Venken, L.; Eberle, W.; Vanderleyden, J. Design and Construction of a Whole Cell Bacterial 4-Hydroxyphenylacetic Acid and 2-Phenylacetic Acid Bioassay. *Front. Bioeng. Biotechnol.* **2015**, *3*, 88.

(18) Ruff, A. Redox polymers in bioelectrochemistry: Common playgrounds and novel concepts. *Curr. Opin. Electrochem.* **2017**, *5*, 66–73.

(19) Thotsaporn, K.; Sucharitakul, J.; Wongratana, J.; Suadee, C.; Chaiyen, P. Cloning and expression of p-hydroxyphenylacetate 3-hydroxylase from Acinetobacter baumannii: Evidence of the divergence of enzymes in the class of two-protein component aromatic hydroxylases. *Biochim. Biophys. Acta, Gene Struct. Expression* **2004**, *1680*, 60–66.

(20) Chaiyen, P.; Suadee, C.; Wilairat, P. A novel two-protein component flavoprotein hydroxylase. *Eur. J. Biochem.* **2001**, *268*, 5550–5561.

DOI: 10.1021/acssensors.9b00144
ACS Sens. 2019, 4, 1270–1278

(21) Teanphonkrang, S.; Janke, S.; Chaiyen, P.; Sucharitakul, J.; Suginta, W.; Khunkaewla, P.; Schuhmann, W.; Ruff, A.; Schulte, A. Tuned Amperometric Detection of Reduced β-Nicotinamide Adenine Dinucleotide by Allosteric Modulation of the Reductase Component of the *p*-Hydroxyphenylacetate Hydroxylase Immobilized within a Redox Polymer. *Anal. Chem.* **2018**, *90*, 5703−5711.
(22) Sucharitakul, J.; Chaiyen, P.; Entsch, B.; Ballou, D. P. The reductase of p-hydroxyphenylacetate 3-hydroxylase from Acinetobacter baumannii requires *p*-hydroxyphenylacetate for effective catalysis. *Biochemistry* **2005**, *44*, 10434−10442.
(23) Ruff, A.; Szczesny, J.; Marković, N.; Conzuelo, F.; Zacarias, S.; Pereira, I. A. C.; Lubitz, W.; Schuhmann, W. A fully protected hydrogenase/polymer-based bioanode for high-performance hydrogen/glucose biofuel cells. *Nat. Commun.* **2018**, *9*, 3675.
(24) Chenault, H. K.; Whitesides, G. M. Regeneration of nicotinamide cofactors for use in organic synthesis. *Appl. Biochem. Biotechnol.* **1987**, *14*, 147−197.
(25) Rover, L.; Fernandes, J. C.; Neto, G. d. O.; Kubota, L. T.; Katekawa, E.; Serrano, S. H. Study of NADH Stability Using Ultraviolet−Visible Spectrophotometric Analysis and Factorial Design. *Anal. Biochem.* **1998**, *260*, 50−55.
(26) Brooks, T.; Keevil, C. W. A simple artificial urine for the growth of urinary pathogens. *Lett. Appl. Microbiol.* **1997**, *24*, 203−206.
(27) Zuppi, C.; Messana, I.; Forni, F.; Rossi, C.; Pennacchietti, L.; Ferrari, F.; Giardina, B. ^{1}H NMR spectra of normal urines: Reference ranges of the major metabolites. *Clin. Chim. Acta* **1997**, *265*, 85−97.
(28) Zhou, C.; Wang, J.; Li, L.; Wang, R.; Hong, M. A palladium chelating complex of ionic water-soluble nitrogen-containing ligand: The efficient precatalyst for Suzuki−Miyaura reaction in water. *Green Chem.* **2011**, *13*, 2100−2106.
(29) Zafar, M. N.; Wang, X.; Sygmund, C.; Ludwig, R.; Leech, D.; Gorton, L. Electron-transfer studies with a new flavin adenine dinucleotide dependent glucose dehydrogenase and osmium polymers of different redox potentials. *Anal. Chem.* **2012**, *84*, 334−341.

DOI: 10.1021/acssensors.9b00144
ACS Sens. 2019, 4, 1270−1278